Marine Environmental Research 210 (2025) 107354

Contents lists available at ScienceDirect

Marine Environmental Research

journal homepage: www.elsevier.com/locate/marenvrev

Microbial regulation of dissolved organic matter revealed by integrated metabolomics and metagenomics in the World's deepest blue hole

Jiying Pei [a,1,*], Shiguo Chen [b,1], Kefu Yu [a,c,**], Jiayuan Liang [a,***], Ruijie Zhang [a], Penghui Li [d,e], Zhuanghao Hou [f], Liang Fu [g], Honglin Ma [g]

[a] Guangxi Laboratory on the Study of Coral Reefs in the South China Sea, Coral Reef Research Center of China, School of Marine Sciences, Guangxi University, Nanning, 530004, China
[b] School of Resources, Environment and Materials, Guangxi University, Nanning, 530004, China
[c] Southern Marine Science and Engineering Guangdong Laboratory (Guangzhou), Guangzhou, 511458, China
[d] School of Marine Sciences, Sun Yat-sen University, Zhuhai, 519082, China
[e] Southern Marine Science and Engineering Guangdong Laboratory (Zhuhai), Zhuhai, 519082, China
[f] School of Chemistry and Materials Science and National Synchrotron Radiation Laboratory, University of Science and Technology of China, Hefei, 230026, China
[g] Sansha Track Ocean Coral Reef Conservation Research Institute, Sansha, 573199, China

ARTICLE INFO

Keywords:
Dissolved organic matter
Metabolomics
Metagenomics
Oxygen stratification
Blue hole

ABSTRACT

Dissolved organic matter (DOM) is central to marine biogeochemical cycles, with its composition and dynamics closely linked to microbial communities. In oxygen-stratified extreme environments, however, the ecological relationships between DOM and microbes remain insufficiently explored. This study explores the dynamics of DOM and microbial communities in the Sansha Yongle Blue Hole, the world's deepest ocean blue hole, using an integrated metabolomics and metagenomics approach. Our findings elucidate significant alterations in microbial communities and DOM composition in response to variations in oxygen concentrations. Specifically, various DOM components, including dissolved organic sulfur (DOS) and dissolved organic nitrogen (DON), along with a spectrum of small molecule metabolites, were affected by microbial metabolic activities. Higher concentrations of DOS in the anoxic layer were positively correlated with increased sulfur metabolism in microbial communities, whereas lower concentrations of DON in the chemocline were associated with the coupling of nitrification and denitrification processes. Additionally, metabolites such as lipids, amino acids, isovalerylcarnitine, and peptides, associated with microbial physiological functions, energy metabolism, and signal transduction processes, varied with oxygen stratification. These findings contribute to a deeper understanding of the intricate relationships between microbial communities and DOM dynamics in extreme marine environments.

1. Introduction

Dissolved organic matter (DOM) is one of the largest pools of reduced carbon in the ocean, comprising a chemically diverse assemblage of molecules. Its complex composition encompasses thousands of distinct compounds—including amino acids, lipids, carbohydrates, phenolic compounds (Li et al., 2024a), and a wide range of heteroatom-containing molecules such as those dissolved organic sulfur (DOS) and dissolved organic nitrogen (DON) (Gomez-Saez et al., 2021). This molecular heterogeneity imparts diverse chemical reactivities and biological availabilities, allowing DOM to serve as a critical mediator in marine biogeochemical cycles (Hansell et al., 2009). Within DOM, DOS and DON occupy particularly important roles in linking carbon and nutrient cycling. DOS serves as both an energy source and a redox-active pool for microorganisms capable of sulfur oxidation and reduction (Tripp et al., 2008). Similarly, DON represents a key nitrogen source for heterotrophic and autotrophic microbes, especially in oligotrophic systems where inorganic nitrogen is limiting (Zehr and Capone, 2020). The

* Corresponding author. Guangxi Laboratory on the Study of Coral Reefs in the South China Sea, Coral Reef Research Center of China, School of Marine Sciences, Guangxi University, Nanning, 530004, China
** Corresponding author.
*** Corresponding author.
E-mail addresses: pjying@gxu.edu.cn (J. Pei), kefuyu@scsio.ac.cn (K. Yu), jyliang@gxu.edu.cn (J. Liang).
[1] Jiying Pei and Shiguo Chen are co-first authors.

https://doi.org/10.1016/j.marenvres.2025.107354
Received 19 March 2025; Received in revised form 13 June 2025; Accepted 8 July 2025
Available online 8 July 2025

bioavailability of DOS and DON depends not only on their molecular structure but also on the functional potential of the microbial communities that utilize them.

Microorganisms are the primary biological agents controlling the turnover and transformation of DOM. Through biosynthetic pathways, heterotrophic degradation, and redox-sensitive transformations, microbial activity modulates DOM quantity, composition, and lability (Kujawinski, 2011; Osterholz et al., 2016). These transformations are not uniform throughout the water column. Instead, they are profoundly influenced by physicochemical gradients, particularly redox conditions (Suominen et al., 2021). In oxygen-depleted or anoxic environments, such as euxinic basins, oxygen minimum zones, and marine blue holes, microbial communities adapt by expressing specialized metabolic pathways including anaerobic respiration, fermentation, sulfur and nitrogen dissimilation, and carbon fixation (Jessen et al., 2017; Patin et al., 2021). As a result, the DOM composition in these systems may reflect a fingerprint of unique microbial metabolisms not observable in surface or well-oxygenated waters. Despite advances in DOM characterization using high-resolution mass spectrometry (Petras et al., 2017), our understanding of the mechanistic links between microbial metabolism and DOM composition—especially under varying redox regimes—remains limited. DOM studies have traditionally focused on bulk measurements (e.g., total dissolved organic carbon (DOC) concentration) or general indicators of lability (e.g., fluorescence indices), which fail to capture the nuanced molecular transformations driven by microbial processes (Bachi et al., 2023; Chaichana et al., 2019).

The Sansha Yongle Blue Hole (SYBH), located in the South China Sea, represents an exceptional natural laboratory to investigate these interactions. As the world's deepest known marine blue hole (>300 m), SYBH exhibits pronounced vertical stratification in oxygen concentration, transitioning from oxygenated surface waters to anoxic and sulfidic conditions below ~90 m (Li et al., 2018; Xie et al., 2019). This strong redox gradient is accompanied by marked shifts in microbial community composition and functional gene abundance with depth (Li et al., 2024b; Zhou et al., 2023). The unique hydrogeological isolation and vertical redox zonation of SYBH make it an ideal site to examine how microbial processes regulate DOM molecular transformations across a natural, chemically stratified water column.

In recent years, advanced analytical tools have emerged to characterize both the microbial and chemical dimensions of such systems. Exometabolomics, the study of extracellular microbial metabolites, allows for direct observation of biologically derived or transformed DOM molecules (Pei et al., 2022a, 2022b, 2024). These methods can detect thousands of mass features, many of which are biologically active or traceable to specific microbial functions. In parallel, shotgun metagenomics provides insight into the taxonomic composition and functional gene repertoire of microbial communities, revealing pathways for carbon, nitrogen, and sulfur metabolism (New and Brito, 2020). While several studies have applied either metagenomics or metabolomics to marine systems, few have integrated both approaches to simultaneously map microbial metabolic potential and the resulting DOM molecular landscape (Pena-Ocana et al., 2022). Such integrative strategies are crucial for disentangling the cause-effect relationships between microbial community composition, metabolic capacity, and DOM chemistry.

In this study, we investigate the microbial regulation of DOM molecular composition across the redox-stratified water column of the SYBH by integrating high-resolution metabolomics and shotgun metagenomics. Our primary objectives are to: 1) Characterize the molecular composition of DOM—including DOS and DON—at multiple depths along the oxygen gradient; 2) Profile the microbial community structure and functional gene distribution across various depths; 3) Identify correlations between microbial metabolic pathways and specific DOM compound classes, with particular focus on sulfur and nitrogen cycling. We hypothesize that microbial communities exert depth-dependent control over DOM composition through selective degradation, transformation, and biosynthesis processes that are closely aligned with local redox conditions and nutrient availability. Specifically, we propose that the dominance of anaerobic pathways in anoxic zones will correlate with distinct signatures in DOM composition, particularly in the DOS and DON pools. Through this integrative analysis, we aim to bridge the gap between microbial ecology and DOM biogeochemistry, offering novel insights into the controls on carbon and nutrient cycling in extreme marine environments.

2. Materials and methods

2.1. Sample collection

The SYBH is situated within the intertidal reef platform of the eastern Yongle atoll in the South China Sea (111.768°E, 16.525°N) (Fig. 1a and b). In October 2019, a total of 28 seawater samples were systematically collected from different depths within the SYBH (0 m, 10 m, 20 m, 50 m, 80 m, 85 m, 90 m, 95 m, 100 m, 110 m, 120 m, 150 m, 200 m, and 250 m) (Fig. 1c). Two duplicate samples were obtained at each depth. Sampling above 190 m was conducted using a conductivity-temperature-depth (CTD) system equipped with rosette samplers, while sampling below 190 m was performed with a remotely operated vehicle (ROV) equipped with a home-made sampler. Environmental parameters, including temperature, salinity, dissolved oxygen (DO), pH, turbidity, and chlorophyll-a (Chl-a), were measured in situ across the 0–300 m depth range using the CTD system mounted on the ROV. Additionally, two additional seawater samples were collected at the reference point on the outer reef slope of Yongle Atoll (111.799°E, 16.534°N) to compare the DOM composition with that of the SYBH. Water samples for DOM analysis and metagenomic analysis were treated in situ. Further details of the sampling and in situ treatment methods can be found in Text S1.

2.2. Solid phase extraction

The solid-phase extraction (SPE)-DOM method followed the procedure developed by Dittmar (Dittmar et al., 2008). Briefly, the filtered seawater samples (1.2 L) were acidified with HCl to pH = 2 and then extracted using Agilent Bond Elut PPL cartridges (200 mg, 3 mL). The cartridges were pre-conditioned with 8 mL of methanol and 8 mL of acidified Milli-Q water (pH = 2) sequentially. Then, seawater was loaded onto the cartridges at a flow rate of 4 mL/min, followed by a wash with 10 mL of acidified Milli-Q water. The sorbents were dried using nitrogen gas, and the adsorbed DOM was eluted with 8 mL of methanol. The eluent was dried to a volume of 0.5 mL using nitrogen gas, and then reconstituted with 0.5 mL of Milli-Q water (1:1 v/v). The extract was stored at −20 °C until liquid chromatography tandem mass spectrometry (LC-MS/MS) analysis.

2.3. LC-MS/MS data acquisition and pre-processing

The DOM extracts were analyzed using a Thermo Q-Exactive mass spectrometer coupled to a Dionex Ulti-Mate 3000 UHPLC system. The chromatographic separation involved methanol and water as mobile phases, with a gradient shift from 5 % to 95 % methanol over 20 min, followed by a 5-min maintenance period. Mass spectrometry data acquisition occurred in positive electrospray ionization (ESI) mode using data-dependent acquisition (DDA). Chromatographic peak extraction from raw mass spectrometry data was conducted using the open-source MZmine software (version 3.4.27) (Heuckeroth et al., 2024). Detailed LC-MS/MS parameters and MZmine extraction parameters can be found in Text S2 and Text S3, respectively. To account for differences in total ion signal across samples, each feature was normalized by dividing its peak intensity by the total ion intensity of all features within the same sample.

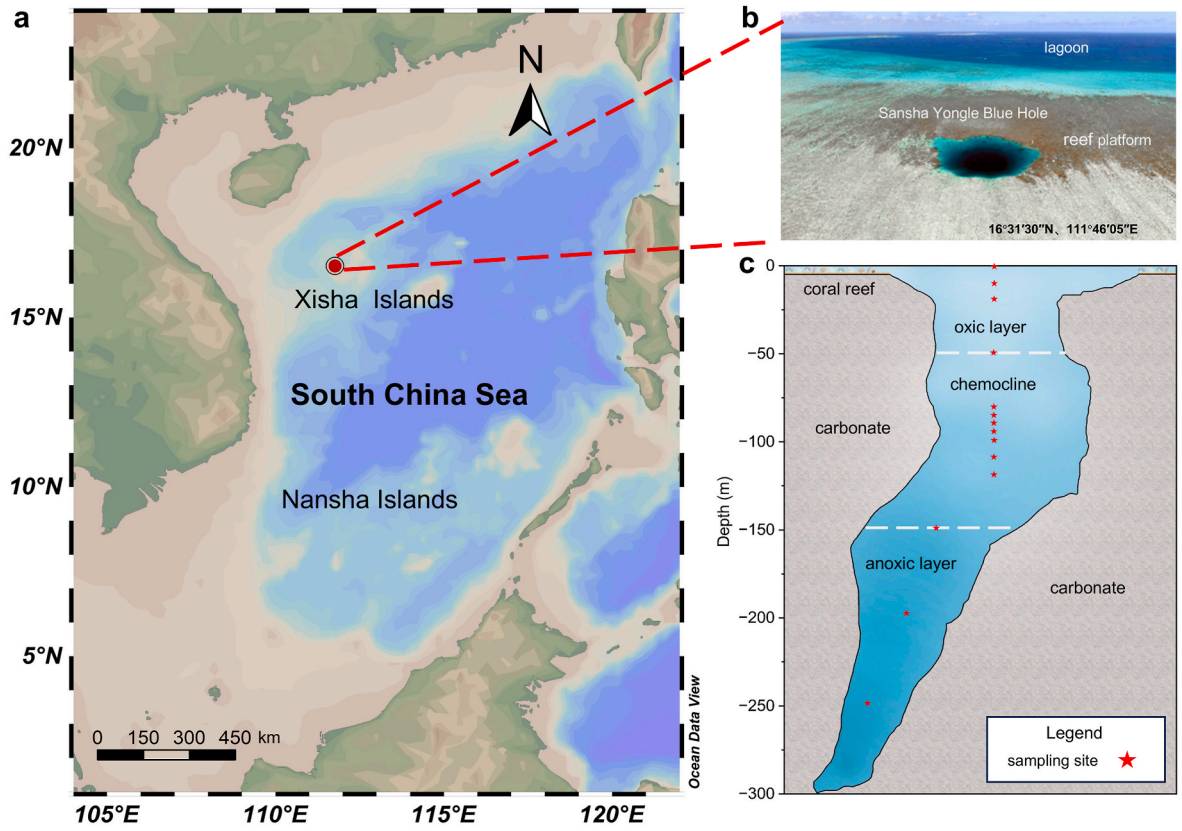

Fig. 1. (a) Map depicting the study area. (b) Realistic depiction of the SYBH located within the reef platform of Yongle Atoll, Xisha Islands. (c) Cross-sectional view of the SYBH and the sampling depths.

2.4. Molecular formula assignment and compound identification

The LC-MS/MS data, exported from MZmine software, underwent molecular formula assignment using the SIRIUS computational annotation tool (version 5.6.3) (Duhrkop et al., 2019). This annotation process involved determining molecular formulas, accurate mass calculation, matching of experimental and predicted isotopic patterns, and analysis of fragmentation trees of the fragment ions, with specific parameters detailed in Text S4. Molecules were classified as DON or DOS based on their molecular formulas, with compounds containing at least one nitrogen or sulfur atom designated as DON or DOS, respectively. Molecules containing both nitrogen and sulfur were included in both categories, reflecting their dual roles in the DOM pool. The relative concentrations of DON and DOS were estimated semi-quantitatively by summing the normalized ion intensities of all identified DON or DOS molecules within each sample. This approach expresses the abundance of each category as a proportion of total detected DOM ion intensity. To assess potential biases toward specific ionized DOM molecules, the ion feature-standardized score (z-score) was calculated. This approach minimized bias arising from variable ionization efficiencies and enabled a more accurate comparison of relative DOM concentrations across samples (Fig. S1).

Compound identification was conducted using the Feature-based Molecular Networking (FBMN) module on the Global Natural Product Social Molecular Networking (GNPS) website. Molecular networking operates on the principle that compounds with similar structures produce similar fragments in their MS/MS spectra (Chung et al., 2021). The structural similarity, quantified by cosine values in the comparison of similar MS/MS spectra (Text S5), facilitates effective inference of the structures of unknown compounds. FBMN analysis for the SYBH dataset was conducted with specific parameters outlined in Text S6. Leveraging the annotated compounds identified via the GNPS library search as "seeds", additional unknown compounds were deduced through manual interpretation. The resulting annotated compounds underwent validation by cross-checking against spectra observed in various databases, including MassBank Europe, MassBank of North America, Metlin, HMDB, and mzCloud. To visualize the output files generated from the FBMN analysis, Cytoscape was utilized (version 3.8.0) (Shannon et al., 2003).

2.5. Microbial DNA extraction and metagenomic analysis

Aseptic forceps were utilized to carefully section the filter membrane containing microorganisms from the frozen storage tube. Subsequently, the FastDNA Spin Kit for Soil was employed to extract total microbial DNA from the filter membrane, preparing it for metagenomic sequencing analysis. The DNA libraries were sequenced on the illumina platform. Subsequently, MEGAHIT software (version 1.1.2) was used for metagenome assembly, with a filter applied to contig sequences shorter than 300 bp (Li et al., 2015). Assembly results were evaluated using QUAST software (version 2.3) (Gurevich et al., 2013). To identify coding regions in the genome, MetaGeneMark software (version 3.26) available at http://exon.gatech.edu/meta_gmhmmp.cgi was utilized (Zhu et al., 2010). Redundancy was removed using cd-hit software (version 4.6.6) at http://www.bioinformatics.org/cd-hit/with a similarity threshold set at 95 % and a coverage threshold at 90 % (Fu et al., 2012). BLAST comparisons were conducted between non-redundant protein sequences and the protein sequences cataloged in the KEGG database for corresponding gene functional annotations. Additionally, sequence comparisons were performed against the species information in the Nr database to obtain insights into sample species composition and relative abundance.

2.6. Quality control

To ensure the reliability of subsequent analysis, for the LC-MS/MS analysis of seawater samples, a comprehensive quality control protocol was implemented, encompassing sample pretreatment, instrument detection, and data analysis. This protocol included a blank control experiment conducted for SPE analysis, a quality control sample prepared from the 14 seawater samples to monitor the stability of the pretreatment and instrument analysis process, a blank experiment to assess instrument pollution, and the use of internal standards to calibrate instrument fluctuations. For a detailed description of the process, refer to Text S7. Raw reads obtained from sequencing were filtered to remove low-quality sequences. This essential step was performed using the software Trimmomatic (version 0.33) (Bolger et al., 2014), which generated clean tags with improved sequencing quality. The relative standard deviation (RSD) of microbial abundance and peak area of DOM in the duplicate samples across various layers ranged from 9.3 % to 17.4 % and from 7.3 % to 13.5 %, respectively (Fig. S2).

2.7. Statistical analysis

Statistical significance was determined using SPSS software (version 23) with a significance threshold set at $p < 0.05$. Normality was assessed using the Shapiro-Wilk test, and an independent sample *t*-test was applied for data with a normal distribution. Alternatively, the Mann-Whitney *U* test was employed for non-normally distributed data. A Venn plot was generated using Venny 2.1 (https://bioinfogp.cnb.csic.es/tools/venny/). Redundancy analysis was conducted using R packages. For multi-omics analysis, Data Integration Analysis for Biomarker discovery using Latent cOmponents (DIABLO) was performed with the mixOmics package (Singh et al., 2019), diagnostic plots and sample plots from multiblock sparse partial least squares discriminant analysis (sPLS-DA) were applied to the correlation study. The microbial taxa at the order level, comprising the top 28 weighted species selected based on model accuracy, were visualized through correlation circles. Other statistical analyses, unless specified, were conducted using Origin software (version 2024).

3. Results

3.1. Physicochemical properties of the SYBH

The aquatic physicochemical parameters within the SYBH exhibited a distinct stratified structure (Fig. 2). Notably, temperature, DO and pH consistently decreased with increasing depth, while salinity and turbidity showed an upward trend. Significant fluctuations of these parameters were observed at depths of 30 m, 50 m, 90 m, and 150 m. For example, at a depth of 50 m, there was a drastic decrease in temperature, DO, and pH, accompanied by a simultaneous increase in salinity. At a depth of 90 m, the oxygen concentration dramatically dropped to zero. At the depth of 150 m, while temperature, salinity, DO, and pH showed minimal change, there was a drastic increase in turbidity. According to these physicochemical parameters, the SYBH water column could therefore be categorized into three layers: the oxic layer (<50 m), the chemocline (50–150 m), and the anoxic layer (150–300 m).

3.2. Chemical diversity and vertical distribution of DOM

A total of 4568 DOM features were extracted from the mass spectrometry dataset for water samples collected from the 14 layers. Among these, 1235 (27.03 %) were present in all three layers, while 289, 946, and 232 molecules were unique to the oxic layer, chemocline, and anoxic layer, respectively (Fig. 3a). Compared to a reference open-ocean site, SYBH exhibited 2048 additional DOM molecules. On average, 1929, 1934, and 1473 DOM molecules were detected in the oxic, chemocline, and anoxic layers, respectively, with corresponding Shannon indices of 8.59, 8.73, and 8.38 (Fig. 3b). A positive correlation was observed between molecular richness and Shannon index (Fig. 3c). Statistically significant differences in both metrics were found between the chemocline and anoxic layer ($p < 0.05$), but not between the oxic layer and chemocline ($p > 0.05$) (Fig. S3). Principal coordinates analysis (PCoA) and orthogonal partial least squares discriminant analysis (OPLS-DA) showed a clear separation of DOM profiles, especially between the anoxic layer and the other two (Fig. 3d, Fig. S4). A total of 198, 322, and 444 differential molecules were identified between the oxic vs. chemocline, oxic vs. anoxic, and chemocline vs. anoxic comparisons, respectively (Fig. S5).

Out of 4568 DOM molecules, SIRIUS predicted 3574 high-quality

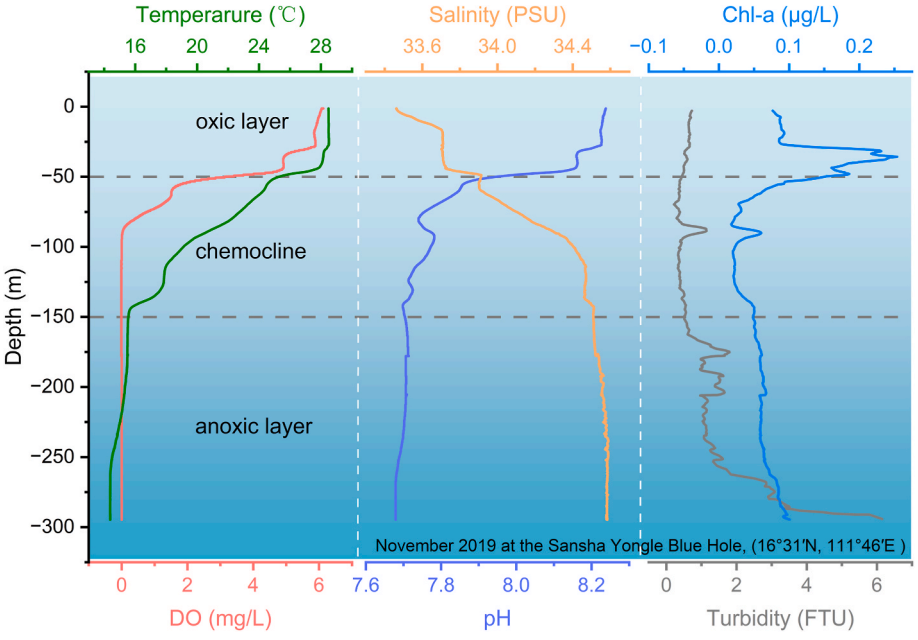

Fig. 2. Variations in physicochemical properties (temperature, DO, salinity, pH, Chl-a, and turbidity at different depths within the SYBH.

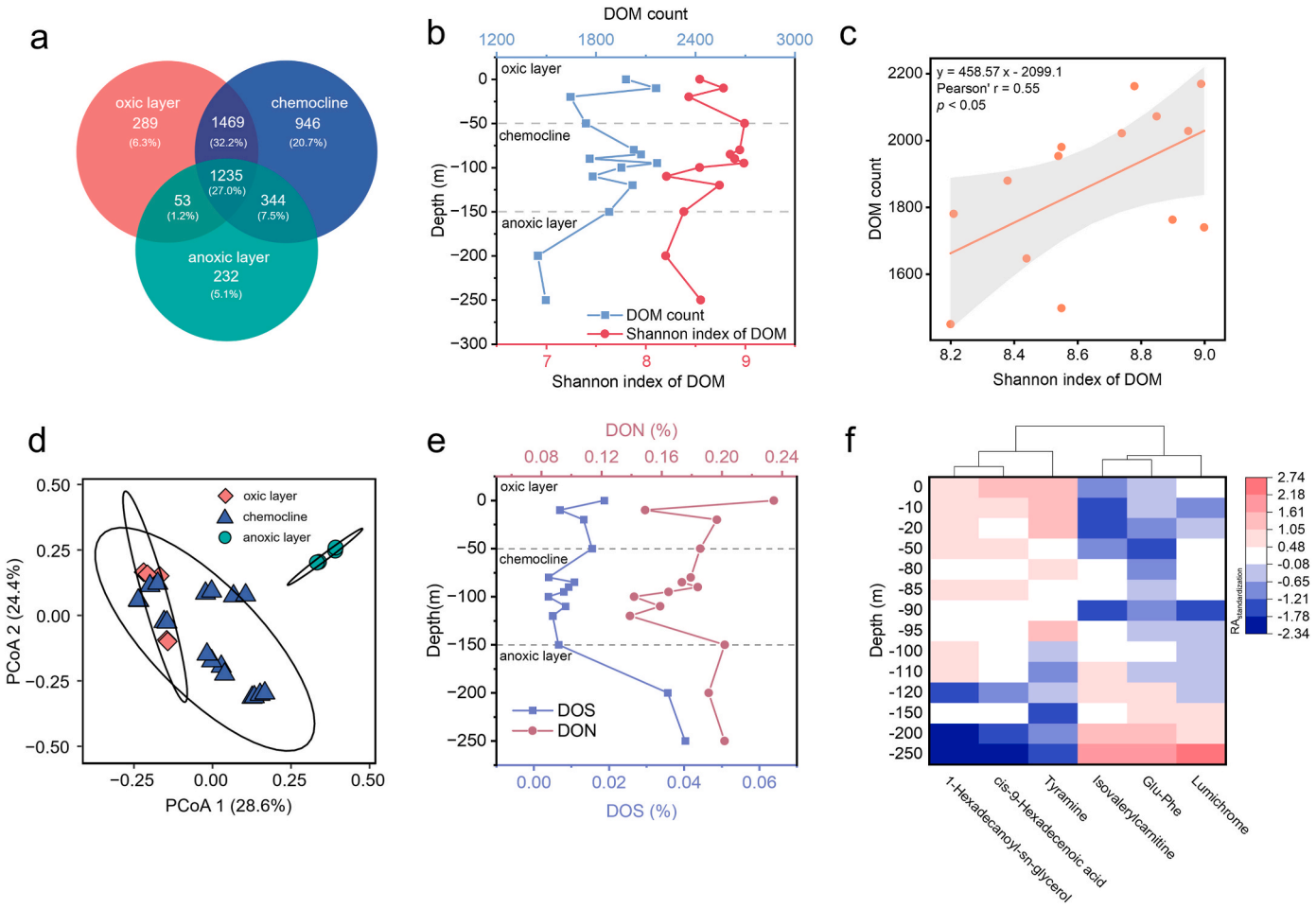

Fig. 3. (a) Venn plot illustrating the distribution of DOM within the oxic layer, chemocline, and anoxic layer of the SYBH. (b) Plot displaying the variation of the DOM count and Shannon index across different depths. (c) Linear correlation analysis between the DOM count and the Shannon index of DOM across different depths. (d) PCoA plot for distinguishing samples from the oxic, chemocline, and the anoxic layer. (e) Variation in the relative abundance of ion peak areas for DOS and DON at different depths within the SYBH. (f) Heatmap depicting the distribution of differential metabolites across different depths.

molecular formulas, including 125 DOS and 1194 DON compounds. DOS concentrations were highest in the anoxic layer, with comparable concentrations in the oxic layer and chemocline, while DON levels were comparable between the oxic and anoxic layers but lower in the chemocline (Fig. 3e). GNPS-based annotation identified 147 DOM molecules, and molecular networking deduced 128 additional structures, totaling 275 annotated compounds. The analysis of differential DOM molecules among the three layers ($p < 0.05$) revealed distinct vertical distribution patterns. Tyramine, cis-9-hexadecenoic acid, and 1-hexadecanoyl-sn-glycerol were primarily enriched in the oxic layer and chemocline, whereas lumichrome, Glu-Phe, and isovalerylcarnitine were predominant in the anoxic layer (Fig. 3f, Fig. S6). These identifications were confidently identified using spectral library matching, with cosine similarity scores ranging from 0.70 to 0.99 (Fig. S7).

3.3. Microbial community and functional analysis

Metagenomic data, described in Table S1 revealed high-quality results with Q30 (%) values exceeding 91 % across all samples. The N50 length ranged from 1006 to 4067, and gene counts varied between 330,686 and 880,209, indicating that the data were robust and suitable for further analysis. To assess microbial diversity, the Shannon index was calculated for each layer in the SYBH. The mean Shannon indices were 4.27 for the oxic layer, 5.03 for the chemocline, and 4.39 for the anoxic layer, with a significant difference observed between the oxic layer and chemocline, but no significant difference between the chemocline and anoxic layer (Fig. 4a). Multivariate statistical analyses, encompassing principal components analysis (PCA) (Fig. 4b) and OPLS-DA (Fig. S8), were employed to investigate water stratification across the 14 layers of the SYBH based on microbial profiling. The results revealed a distinct separation of samples from the oxic layer, chemocline, and anoxic layer. Redundancy analysis (RDA) indicated that DO significantly influenced microbial communities, comparable to the effects of temperature and salinity (Fig. 4c).

Microbial community composition analysis indicated that orders characterized by a higher diversity of anaerobic and microaerophilic species, such as Desulfobacterales and Thiotrichales were more abundant in the anoxic layer (Fig. 4d, Fig. S9a and b). Conversely, aerobic species orders, such as Rhodobacterales and Rhizobiales, associated with nitrogen metabolism, were more prevalent in the oxic layer (Fig. 4d). Notably, nitrifying bacteria orders and denitrifying bacteria orders, including Nitrosopumilales, Nitrosomonadales and Planctomycetales, were concentrated in the chemocline (Fig. S9c and d).

Metabolic functions of microbial communities were annotated against the KEGG metabolic pathway database, identifying 174 metabolic pathways. Statistical analysis revealed 12 pathways with significant differences between the oxic and anoxic layers ($p < 0.05$). Examination of these pathways across various depths (Fig. 4e) showed that energy metabolism and signal transduction were more abundant in the anoxic layer. Conversely, pathways related to the metabolism of cofactors and vitamins, nucleotide metabolism, amino acid metabolism, carbohydrate metabolism, xenobiotics biodegradation, lipid

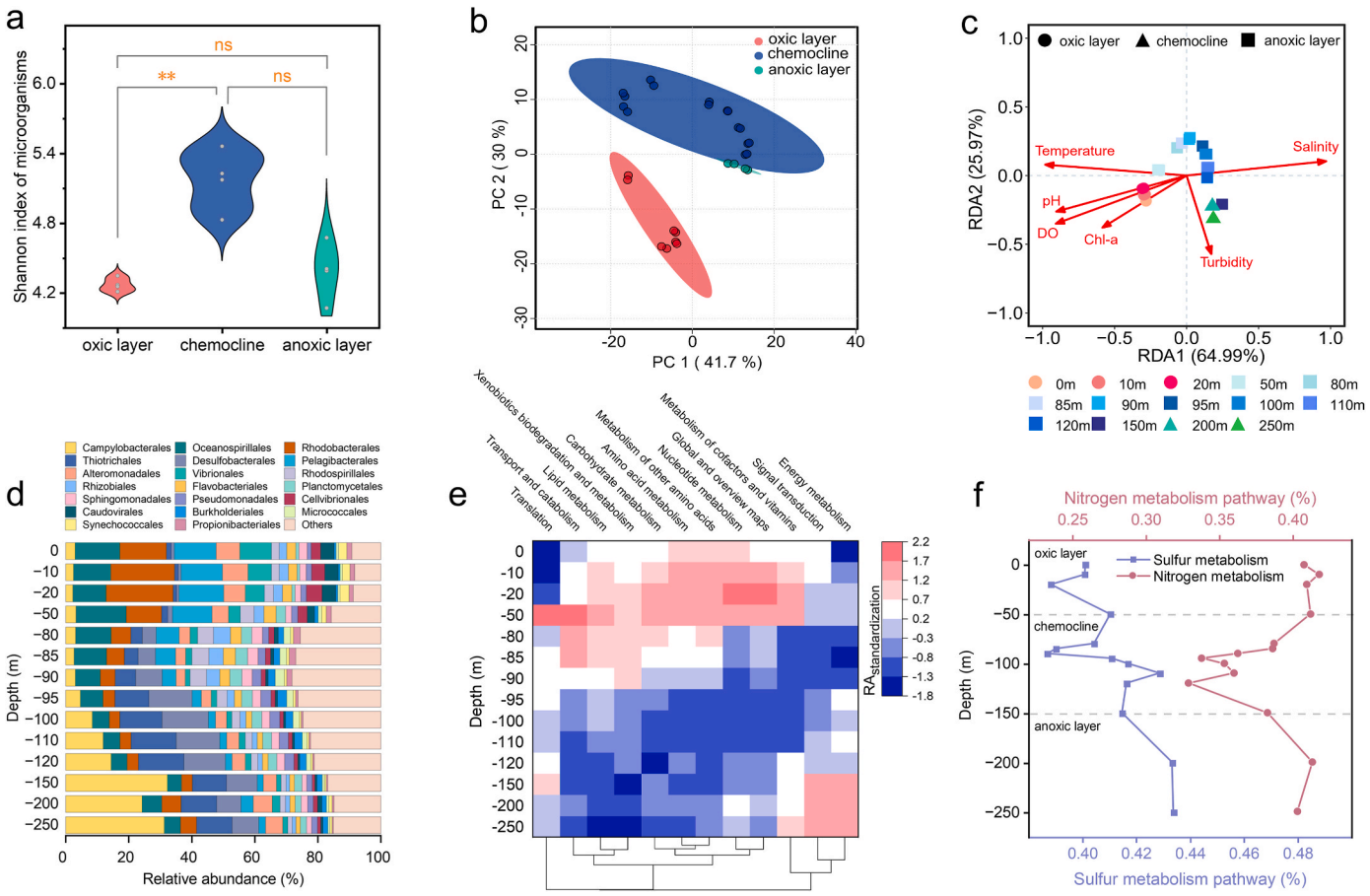

Fig. 4. (a) Violin plot depicting the Shannon index of microorganisms in the oxic layer, chemocline, and anoxic layer within the SYBH. (b) PCA plot for distinguishing samples from the oxic, chemocline, and the anoxic layer. (c) RDA plot showing the relationship between environmental factors and microbial community composition. (d) Relative abundance of microorganisms at the order level across different layers. (e) Heatmap displaying the distribution of metabolic pathways of microorganisms across different depths. (f) Variation of the relative abundance of sulfur metabolism and nitrogen metabolism across different depths.

metabolism, and translation were more prominent in the oxic layer. Sulfur metabolism exhibited a higher relative abundance in the anoxic layer compared to the oxic layer (Fig. 4f), especially in modules like assimilatory sulfate reduction (M00176) (Fig. S10a) and thiosulfate oxidation by the SOX complex (M00595) (Fig. S10b). Nitrogen metabolism's relative abundance was similar between the oxic and anoxic layers but significantly lower in the chemocline (Fig. 4f). Notably, the nitrification module, denitrification module (Fig. S11a and b) and nitrogen fixation-related genes and nifH were most prevalent in the anoxic layer (Fig. S11c and d).

3.4. Correlation analysis between DOM and microbial communities

To explore the relationship between DOM and microbial communities across redox gradients in SYBH, multivariate correlation analyses were conducted. MixOmics analysis revealed strong correlations between the distribution of DOM and microorganisms (Fig. 5a), with an R-value of 0.94. Consistently, sPLS-DA plots showed a consistent distribution trend of DOM with microorganisms across the oxic layer, chemocline, and anoxic layer (Fig. 5b and c). Further analysis showed a significant positive correlation ($p < 0.05$) between DOM molecular diversity and microbial diversity (Fig. 5d), both of which peaked in the chemocline zone (Fig. S12). This pattern indicates that redox transitions may shape both chemical and biological complexity. Furthermore, DOM elemental composition was closely linked to microbial metabolic potential: concentrations of DOS showed a significant positive correlation ($p < 0.05$) with the abundance of genes involved in sulfur metabolism, while DON was positively correlated ($p < 0.05$) with nitrogen metabolism-related gene abundance (Fig. 5e and f).

At the taxon-metabolite level, distinct associations were identified across redox zones (Fig. 5g). In the oxic layer, aerobic bacteria including Puniceicoccales, Oceanospirillales, Pelagibacterales, and Arenicellales were associated with metabolites such as 1-hexadecanoyl-sn-glycerol, cis-9-hexadecenoic acid, and tyramine. In contrast, anaerobic taxa such as Candidatus Altiarchaeares and Thermodesulfobacteriales in the anoxic layer were correlated with isovalerylcarnitine, lumichrome, and Glu-Phe. Microbial responses to different redox environments may be reflected in the activity of key metabolic enzymes. Notably, a significant negative correlation ($p < 0.05$) was observed between the relative abundance of isovaleryl-CoA dehydrogenase and the concentration of isovalerylcarnitine in the water column (Fig. 5h). This suggests that the accumulation of isovalerylcarnitine may be linked to reduced expression of its associated catabolic enzyme under anoxic conditions.

4. Discussion

4.1. Environmental influences on microbial diversity

In marine ecosystems, environmental conditions intricately shape microbial community composition. In the SYBH, a distinct thermohaline gradient forms within the chemocline, limiting upper and lower water layer mixing (Fig. 2). This gradient creates significant variations in DO, temperature, salinity, pH, Chl-a, and turbidity along the water column, creating distinct ecological niches for microbial communities. The RDA analysis (Fig. 4c) revealed that microbial community composition was significantly influenced by these environmental factors. Samples from

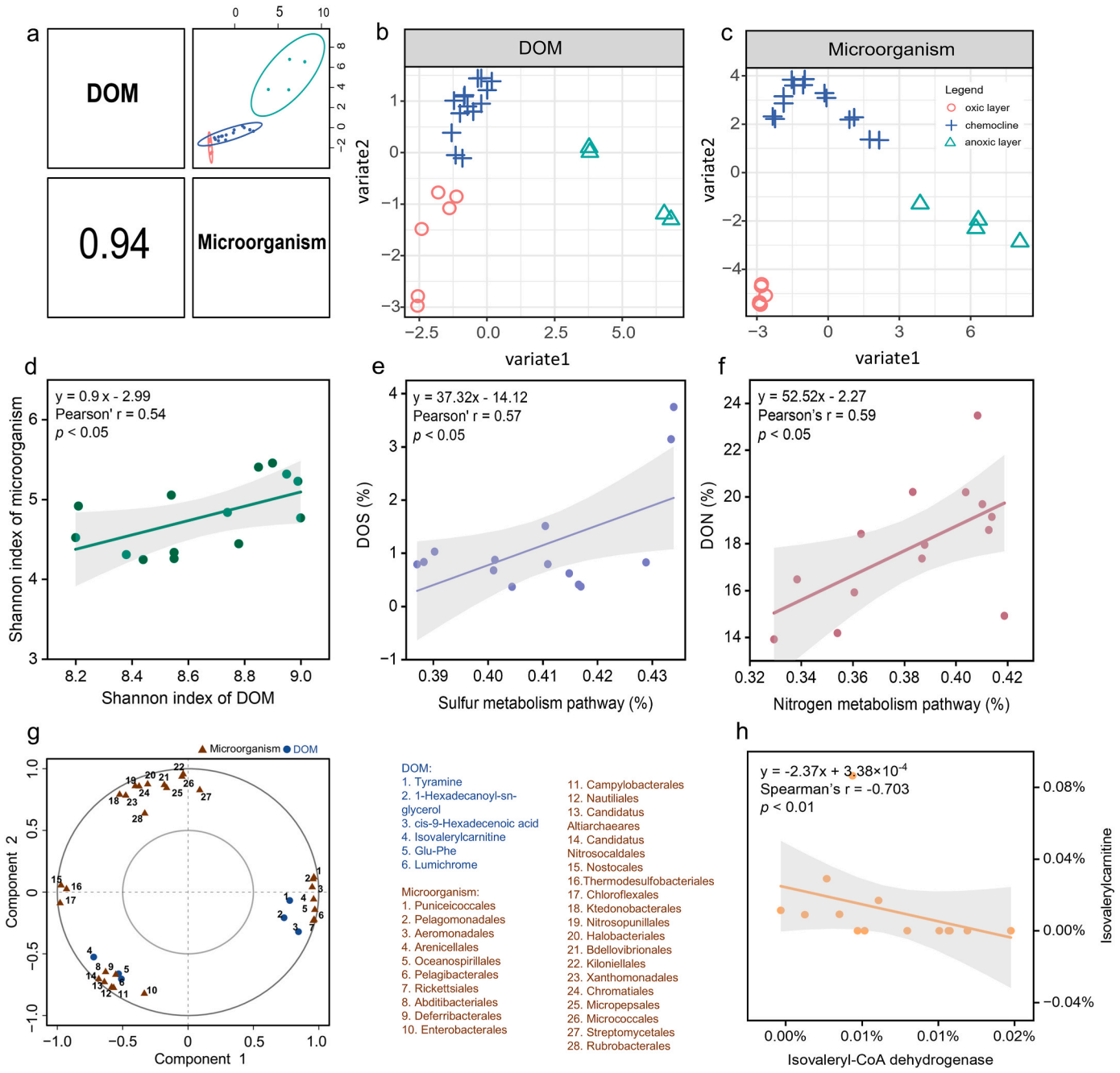

Fig. 5. (a) Score plot from DIABLO analysis. Multiblock sPLS-DA plots illustrating clear separation of samples from the oxic layer, chemocline, and anoxic layer based on (b) metabolomics and (c) metagenomics profiles. (d) Correlation between the Shannon diversity index of DOM and microbial communities, emphasizing compositional coupling across depths. Linear correlations between the relative abundance of DOM ion peaks and microbial functional groups, highlighting the associations between (e) DOS and sulfur metabolism, and (f) DON and nitrogen metabolism. (g) Correlation circle plot derived from multiblock sPLS-DA analysis conducted on DOM and microorganism datasets. (h) Positive correlation between the abundance of isovaleryl-CoA dehydrogenase and isovalerylcarnitine, suggesting microbial mediation of energy-related metabolites.

the oxic layer were positively associated with DO, pH, and Chl-a. High DO supports aerobic taxa such as Oceanospirillales, while elevated Chl-a indicates increased primary productivity, which provides organic matter to fuel heterotrophic microbial activity. In contrast, microbial communities in the anoxic layer were more strongly associated with turbidity. Elevated turbidity often reflects higher levels of suspended particles, which can serve as attachment surfaces and nutrient sources for anaerobic microbes such as Desulfobacterales (Ma et al., 2024).These patterns are consistent with findings from other marine environments. For example, Jessen et al. reported that oxygen gradients in the Black Sea significantly shaped microbial community structure and ecosystem function (Jessen et al., 2017). Abirami et al. observed that microbial communities adapt to various physicochemical factors, including temperature and nutrient availability (Abirami et al., 2021). Similarly, Zaikova et al. found increased microbial diversity in the hypoxic transition zone of Saanich Inlet compared to deeper anoxic waters (Zaikova et al., 2010). Together, these results suggest that the microbial community structure in the SYBH is shaped by environmental gradients and the adaptive responses of microbes to changing redox and physicochemical conditions across the water column.

4.2. Microorganism-regulated metabolism in SYBH

In the ocean, DOM experiences dynamic changes influenced by microorganisms through metabolic pathways such as production (LaBrie et al., 2022), degradation (Xiao et al., 2022), and transformation (Xiao et al., 2023). This microbial regulation establishes a strong correlation between DOM diversity and microbial diversity (Chen et al., 2022; Suominen et al., 2021). Moreover, even within a single microorganism, specific environmental conditions can induce diverse metabolic pathways. This adaptability and specialization of microbial species to their environmental conditions enhance the repertoire of metabolites they produce (Doi, 2018). Consequently, the varied microbial diversity and metabolic pathways in the SYBH contribute to the abundance and diversity of DOM observed in this oxygen-stratified environment.

4.2.1. Microorganism-regulated sulfur metabolism in SYBH

Microbial-regulated sulfur metabolism is integral to the biogeochemical cycles of DOS, vital for global climate regulation (Ksionzek et al., 2016). In the SYBH, DOS shows a pronounced vertical gradient, with notably lower concentrations in the oxic layer and chemocline compared to deeper layers. This depletion is likely due to enhanced microbial remineralization of DOS in oxygen-rich environments. Compared to DOC, DOS is more chemically reactive and thus more prone to microbial degradation during its vertical transport from surface to depth (Tang and Liu, 2023). This observation is consistent with patterns reported in the North Atlantic Deep Water, where aging waters exhibit a decline in total organic sulfur while DOC remains relatively stable (Longnecker et al., 2020). These findings suggest that microbial activity in surface and mid-depth waters accelerates DOS turnover, contributing to its reduced presence in the upper water column of SYBH.

In contrast, DOS concentrations increase in the anoxic bottom layers of SYBH, likely due to both microbial and abiotic processes. Microbial community analysis revealed a higher relative abundance of sulfur-reducing microorganisms in the anoxic zone compared to oxic layers, including Desulfobacterales, Desulfovibrionales, Thermodesulfobacteriales, and Desulfuromonadales (Fig. S9a). These taxa are typical sulfate-reducing bacteria (SRB), capable of using inorganic sulfate (SO_4^{2-}) as terminal electron acceptors, producing hydrogen sulfide (H_2S) as a byproduct. The dominance of Desulfobacterales, in particular, reflects strong adaptation to the anoxic conditions in SYBH. The accumulation of H_2S in the anoxic bottom waters (Yao et al., 2020) is consistent with both the elevated abundance of sulfate-reduction genes (Fig. S10a) and the activity of SRB. Furthermore, H_2S can participate in abiotic reactions with DOM, promoting the formation of new DOS compounds. This mechanism has been observed in other anoxic marine systems, such as the Black Sea and shallow hydrothermal vents, where non-biological interactions between H_2S and organic matter contribute to DOS production (Gomez-Saez et al., 2021). Together, these findings indicate that DOS dynamics in SYBH are shaped by a dual mechanism: microbial remineralization dominates in the oxygenated upper layers, while microbial sulfate reduction and H_2S-mediated DOS formation drive DOS accumulation in the anoxic bottom waters.

4.2.2. Microorganism-regulated nitrogen metabolism in SYBH

The vertical distribution of DON within the SYBH is influenced by microbial metabolism. In the oxygen-rich layers of SYBH, prevalent nitrogen-fixing bacteria convert atmospheric N_2 into bioavailable forms, primarily ammonia nitrogen. This ammonia nitrogen is further metabolized into organic nitrogen, actively contributing to DON cycling in the surface marine environment (Letscher et al., 2013; McCarthy et al., 2004). As depth increases within SYBH, organic matter undergoes oxidation and decomposition, converting organic nitrogen into ammonia (Chen et al., 2023). The chemocline of SYBH, acting as the boundary between the oxic and anoxic regions, provides conditions for the simultaneous occurrence of aerobic nitrification and anaerobic denitrification processes in its micro-oxic environment. This study suggests that the decrease in the relative abundance of DON is closely related to the coupled nitrification-denitrification process. In this process, DON is first decomposed by heterotrophic microorganisms into ammonia, which is then converted into nitrate by nitrifying bacteria. Subsequently, in local anoxic microenvironments, denitrifying bacteria reduce the nitrate to gaseous nitrogen (Ji et al., 2018). This coupled process accelerates the mineralization of DON and the removal of nitrogen through the continuous conversion pathway of "DON → ammonia → nitrate → gaseous nitrogen" ultimately causing it to escape the system in gaseous form, resulting in a decrease in DON accumulation in the chemocline, a higher relative abundance of functional genes related to nitrification and denitrification was observed (Fig. S11a and b). At the same time, a large number of nitrifying microorganisms capable of converting ammonia to nitrite were present (including Nitrosopumilales, Nitrosomonadales, Nitrospinales, Nitrospirales, and Cenarchaeales), as well as denitrifying microorganisms including Planctomycetales, Xanthomonadales, Hydrogenophilales, and Pseudomonadales (Fig. S9c and d), further confirming the above inference.

Conversely, the increase in DON concentrations in the anoxic layer of the SYBH compared to the chemocline is associated with anaerobic microbial nitrogen fixation. This is supported by the observed increase in nitrogenase content within the anoxic layer, where nitrogenase facilitates nitrogen fixation under low-oxygen conditions (Bauersachs et al., 2010; Yin et al., 2023). Additionally, the increased abundance of modules related to nitrogen fixation (Fig. S11c), along with a heightened presence of the nifH gene (Fig. S11d), associated with various nitrogen-fixing bacteria, underscores the significant role of microbial nitrogen fixation in augmenting DON concentrations in this anoxic environment. The nitrogen in the anoxic layer of the SYBH may originate from microbial denitrification or anammox processes, sustaining the availability of nitrogen for nitrogen-fixing bacteria to continue contributing to the DON pool.

4.3. Other microorganism-regulated metabolism in SYBH

The microbial community in SYBH produces a diverse array of metabolites involved in energy metabolism and signal transduction. Elevated levels of 1-hexadecanoyl-sn-glycerol and cis-9-hexadecenoic acid in the oxic layer may stem from active microbial lipid metabolism (Liu et al., 2020). Similarly, higher concentrations of tyramine in the oxic layer may suggest active microbial amino acid metabolism. In environments with limited organic carbon, microorganisms may alter their metabolic strategies to support survival. The increased concentrations of isovalerylcarnitine in the anoxic layer of SYBH may enhance microbial metabolic energy utilization efficiency. Isovalerylcarnitine, essential for fatty acid oxidation, aids in breaking down fatty acids for energy production within mitochondria (Rebouche and Seim, 1998). This process relies on the enzyme isovaleryl-CoA dehydrogenase, which is critical for mitochondrial beta-oxidation. Reduced levels of this enzyme in the anoxic layer of SYBH suggest a shift towards optimizing energy generation through enhanced mitochondrial beta-oxidation in response to oxygen depletion, potentially leading to the accumulation of isovalerylcarnitine (Fig. 5e) (Kuhn et al., 2023).

Functional annotation analysis reveals enriched signal transduction processes in the anoxic layer of SYBH (Fig. 4e), indicating the involvement of signal transduction molecules such as Glu-Phe and lumichrome in microbial communication. Previous investigations have shown that cyclic dipeptides signal the transport of peptidases in aerobic, gram-negative bacteria in deep-sea environments (Sun et al., 2020), while lumichrome contributes to biotic signal transduction during biofilm formation (van Galen et al., 2020). These findings suggest that the elevated concentrations of Glu-Phe and lumichrome in the anoxic layer of SYBH are crucial for microbial adaptation in this unique marine environment.

5. Conclusions

Leveraging an integrative approach that intertwines metabolomics and metagenomics, this study conducted an in-depth exploration of DOM diversity, the functional potential of microbial communities, and their ecological roles within the SYBH. A significant correlation between DOM distribution and microbial activity, influenced by environmental factors, notably oxygen concentrations, was observed. Various components of DOM, including DOS and DON, as well as an array of metabolites, were discernibly impacted by the metabolic activities of microorganisms, specifically bacteria associated with sulfur and nitrogen metabolism. The research provides crucial insights into global carbon cycling dynamics through detailed profiling of DOM composition. This improved understanding significantly enhances our grasp of how ecosystems operate in intricate marine environments, particularly those marked by notable fluctuations in oxygen concentration.

CRediT authorship contribution statement

Jiying Pei: Writing – review & editing, Project administration, Methodology, Funding acquisition, Conceptualization. **Shiguo Chen:** Writing – original draft, Visualization, Investigation, Formal analysis. **Kefu Yu:** Resources, Project administration, Funding acquisition. **Jiayuan Liang:** Writing – review & editing, Resources, Methodology, Data curation. **Ruijie Zhang:** Supervision. **Penghui Li:** Methodology. **Zhuanghao Hou:** Software. **Liang Fu:** Resources. **Honglin Ma:** Investigation.

Data availability statement

The raw LC-MS/MS data has been deposited in the Mass Spectrometry Interactive Virtual Environment (http://massive.ucsd.edu/) under the accession number MSV000080562. The raw metagenomic data has been submitted into the NCBI Sequence Read Archive database (https://www.ncbi.nlm.nih.gov/) under the accession numbers PRJNA1201745. The map in Fig. 1a was prepared with the software Ocean Data View (version 5.6.7) (Schlitzer, 2002). The image in Fig. 1b was reproduced from http://www.trackocean.cn/.

Declaration of competing interest

The authors declare that they have no known competing financial interests or personal relationships that could have appeared to influence the work reported in this paper.

Acknowledgments

This work was supported by Guangxi Science and Technology Program (No. AD25069075), Guangxi Natural Science Foundation (Nos. 2023GXNSFAA026488), and National Natural Science Foundation of China (Nos. 22264003 and 42090041).

Appendix A. Supplementary data

Supplementary data to this article can be found online at https://doi.org/10.1016/j.marenvres.2025.107354.

Data availability

Data will be made available on request.

References

Abirami, B., Radhakrishnan, M., Kumaran, S., Wilson, A., 2021. Impacts of global warming on marine microbial communities. Sci. Total Environ. 791, 147905. https://doi.org/10.1016/j.scitotenv.2021.147905.

Bachi, G., Morelli, E., Gonnelli, M., Balestra, C., Casotti, R., Evangelista, V., et al., 2023. Fluorescent properties of marine phytoplankton exudates and lability to marine heterotrophic prokaryotes degradation. Limnol. Oceanogr. 68 (4), 982–1000. https://doi.org/10.1002/lno.12325.

Bauersachs, T., Speelman, E.N., Hopmans, E.C., Reichart, G.J., Schouten, S., Damste, J.S., 2010. Fossilized glycolipids reveal past Oceanic N_2 fixation by heterocystous Cyanobacteria. Proc. Natl. Acad. Sci. U. S. A 107 (45), 19190–19194. https://doi.org/10.1073/pnas.1007526107.

Bolger, A.M., Lohse, M., Usadel, B., 2014. Trimmomatic: a flexible trimmer for illumina sequence data. Bioinformatics 30 (15), 2114–2120. https://doi.org/10.1093/bioinformatics/btu170.

Chaichana, S., Jickells, T., Johnson, M., 2019. Interannual variability in the summer dissolved organic matter inventory of the north sea: implications for the Continental shelf pump. Biogeosciences 16 (5), 1073–1096. https://doi.org/10.5194/bg-16-1073-2019.

Chen, L., Yao, P., Yang, Z., Fu, L., 2023. Seasonal and vertical variations of nutrient cycling in the world's deepest blue hole. Front. Mar. Sci. 10, 1172475. https://doi.org/10.3389/fmars.2023.1172475.

Chen, Q., Lønborg, C., Chen, F., Gonsior, M., Li, Y., Cai, R., et al., 2022. Increased microbial and substrate complexity result in higher molecular diversity of the dissolved organic matter pool. Limnol. Oceanogr. 67 (11), 2360–2373. https://doi.org/10.1002/lno.12206.

Chung, H., Kao, C., Wang, T., Chu, J., Pei, J., Hsu, C., 2021. Reaction tracking and high-throughput screening of active compounds in combinatorial chemistry by tandem mass spectrometry molecular networking. Anal. Chem. 93 (4), 2456–2463. https://doi.org/10.1021/acs.analchem.0c04481.

Dittmar, T., Koch, B., Hertkorn, N., Kattner, G., 2008. A simple and efficient method for the solid-phase extraction of dissolved organic matter (SPE-DOM) from seawater. Limnol Oceanogr. Methods 6, 230–235. https://doi.org/10.4319/lom.2008.6.230.

Doi, Y., 2018. Lactic acid fermentation is the main aerobic metabolic pathway in Enterococcus faecalis metabolizing a high concentration of glycerol. Appl. Microbiol. Biotechnol. 102 (23), 10183–10192. https://doi.org/10.1007/s00253-018-9351-4.

Duhrkop, K., Fleischauer, M., Ludwig, M., Aksenov, A.A., Melnik, A.V., Meusel, M., et al., 2019. Sirius 4: a rapid tool for turning tandem mass spectra into metabolite structure information. Nat. Methods 16 (4), 299–302. https://doi.org/10.1038/s41592-019-0344-8.

Fu, L., Niu, B., Zhu, Z., Wu, S., Li, W., 2012. CD-HIT: accelerated for clustering the next-generation sequencing data. Bioinformatics 28 (23), 3150–3152. https://doi.org/10.1093/bioinformatics/bts565.

Gomez-Saez, G.V., Dittmar, T., Holtappels, M., Pohlabeln, A.M., Lichtschlag, A., Schnetger, B., et al., 2021. Sulfurization of dissolved organic matter in the anoxic water column of the black sea. Sci. Adv. 7 (25), eabf6199. https://doi.org/10.1126/sciadv.abf6199.

Gurevich, A., Saveliev, V., Vyahhi, N., Tesler, G., 2013. QUAST: quality assessment tool for genome assemblies. Bioinformatics 29 (8), 1072–1075. https://doi.org/10.1093/bioinformatics/btt086.

Hansell, D.A., Carlson, C.A., Repeta, D.J., Schlitzer, R., 2009. Dissolved organic matter in the ocean a controversy stimulates new insights. Oceanography (Wash. D. C.) 22 (4), 202–211. https://doi.org/10.5670/oceanog.2009.109.

Heuckeroth, S., Damiani, T., Smirnov, A., Mokshyna, O., Brungs, C., Korf, A., et al., 2024. Reproducible mass spectrometry data processing and compound annotation in MZmine 3. Nat. Protoc. 19 (9), 2597–2641. https://doi.org/10.1038/s41596-024-00996-y.

Jessen, G.L., Lichtschlag, A., Ramette, A., Pantoja, S., Rossel, P.E., Schubert, C.J., et al., 2017. Hypoxia causes preservation of labile organic matter and changes seafloor microbial community composition (black sea). Sci. Adv. 3 (2), e1601897. https://doi.org/10.1126/sciadv.1601897.

Ji, Q., Buitenhuis, E., Suntharalingam, P., Sarmiento, J.L., Ward, B.B., 2018. Global nitrous oxide production determined by oxygen sensitivity of nitrification and denitrification. Glob. Biogeochem. Cycles 32 (12), 1790–1802. https://doi.org/10.1029/2018gb005887.

Ksionzek, K.B., Lechtenfeld, O.J., McCallister, S.L., Schmitt-Kopplin, P., Geuer, J.K., Geibert, W., et al., 2016. Dissolved organic sulfur in the ocean: biogeochemistry of a petagram inventory. Science 354 (6311), 456–459. https://doi.org/10.1126/science.aaf7796.

Kuhn, S., Williams, M.E., Dercksen, M., Sass, J.O., van der Sluis, R., 2023. The glycine N-acyltransferases, GLYAT and GLYATL1, contribute to the detoxification of isovaleryl-CoA - an in-silico and in vitro validation. Comput. Struct. Biotec. 21, 1236–1248. https://doi.org/10.1016/j.csbj.2023.01.041.

Kujawinski, E.B., 2011. The impact of microbial metabolism on marine dissolved organic matter. Ann. Rev. Mar. Sci 3, 567–599. https://doi.org/10.1146/annurev-marine-120308-081003.

LaBrie, R., Péquin, B., St-Gelais, N.F., Yashayaev, I., Cherrier, J., Gélinas, Y., et al., 2022. Deep ocean microbial communities produce more stable dissolved organic matter through the succession of rare prokaryotes. Sci. Adv. 8 (27), eabn0035. https://doi.org/10.1126/sciadv.abn0035.

Letscher, R.T., Hansell, D.A., Carlson, C.A., Lumpkin, R., Knapp, A.N., 2013. Dissolved organic nitrogen in the global surface ocean: distribution and fate. Glob. Biogeochem. Cycles 27 (1), 141–153. https://doi.org/10.1029/2012gb004449.

Li, D., Liu, C.M., Luo, R., Sadakane, K., Lam, T.W., 2015. MEGAHIT: an ultra-fast single-node solution for large and complex metagenomics assembly via succinct de Bruijn graph. Bioinformatics 31 (10), 1674–1676. https://doi.org/10.1093/bioinformatics/btv033.

Li, P., Liang, W., Zhou, Y., Yi, Y., He, C., Shi, Q., et al., 2024a. Hypoxia diversifies molecular composition of dissolved organic matter and enhances preservation of

terrestrial organic carbon in the yangtze river Estuary. Sci. Total Environ. 906, 167661. https://doi.org/10.1016/j.scitotenv.2023.167661.
Li, Q., Lei, Y., Li, T., 2024b. DNA metabarcoding reveals ecological patterns and driving mechanisms of archaeal, bacterial, and eukaryotic communities in sediments of the sansha yongle blue hole. Sci. Rep. 14 (1), 6745. https://doi.org/10.1038/s41598-024-57214-8.
Li, T., Feng, A., Liu, Y., Li, Z., Guo, K., Jiang, W., et al., 2018. Three-dimensional (3D) morphology of sansha yongle blue hole in the South China Sea revealed by underwater remotely operated vehicle. Sci. Rep. 8 (1), 17122. https://doi.org/10.1038/s41598-018-35220-x.
Liu, B., Sun, Y., Hang, W., Wang, X., Xue, J., Ma, R., et al., 2020. Characterization of a novel Acyl-ACP Delta(9) desaturase gene responsible for palmitoleic acid accumulation in a diatom Phaeodactylum tricornutum. Front. Microbiol. 11, 584589. https://doi.org/10.3389/fmicb.2020.584589.
Longnecker, K., Oswald, L., Kido Soule, M.C., Cutter, G.A., Kujawinski, E.B., 2020. Organic sulfur: a spatially variable and understudied component of marine organic matter. Limnol. Oceanogr. Lett. 5 (4), 305–312. https://doi.org/10.1002/lol2.10149.
Ma, J., Wen, L., Li, X., Dai, J., Song, J., Wang, Q., et al., 2024. Different fates of particulate matters driven by marine hypoxia: a case study of oxygen minimum zone in the Western Pacific. Mar. Environ. Res. 200, 106648. https://doi.org/10.1016/j.marenvres.2024.106648.
McCarthy, M.D., Benner, R., Lee, C., Hedges, J.I., Fogel, M.L., 2004. Amino acid carbon isotopic fractionation patterns in Oceanic dissolved organic matter: an unaltered photoautotrophic source for dissolved organic nitrogen in the ocean? Mar. Chem. 92 (1–4), 123–134. https://doi.org/10.1016/j.marchem.2004.06.021.
New, F.N., Brito, I.L., 2020. What is metagenomics teaching Us, and what is missed? Annu. Rev. Microbiol. 74, 117–135. https://doi.org/10.1146/annurev-micro-012520-072314.
Osterholz, H., Singer, G., Wemheuer, B., Daniel, R., Simon, M., Niggemann, J., et al., 2016. Deciphering associations between dissolved organic molecules and bacterial communities in a pelagic marine system. ISME J. 10 (7), 1717–1730. https://doi.org/10.1038/ismej.2015.231.
Patin, N.V., Dietrich, Z.A., Stancil, A., Quinan, M., Beckler, J.S., Hall, E.R., et al., 2021. Gulf of Mexico blue hole harbors high levels of novel microbial lineages. ISME J. 15 (8), 2206–2232. https://doi.org/10.1038/s41396-021-00917-x.
Pei, J., Chen, S., Yu, K., Hu, J., Wang, Y., Zhang, J., et al., 2022a. Metabolomics characterization of Scleractinia corals with different life-history strategies: a case study about *pocillopora Meandrina* and *Seriatopora hystrix* in the South China Sea. Metabolites 12 (11), 1079. https://doi.org/10.3390/metabo12111079.
Pei, J., Yu, W., Zhang, J., Kuo, T., Chung, H., Hu, J., et al., 2022b. Mass spectrometry-based metabolomic signatures of coral bleaching under thermal stress. Anal. Bioanal. Chem. 414 (26), 7635–7646. https://doi.org/10.1007/s00216-022-04294-y.
Pei, J., Zhou, Y., Chen, S., Yu, K., Qin, Z., Zhang, R., et al., 2024. Chemical diversity of scleractinian corals revealed by untargeted metabolomics and molecular networking. Acta Oceanol. Sin. 42 (11), 127–135. https://doi.org/10.1007/s13131-023-2173-y.
Pena-Ocana, B.A., Ovando-Ovando, C.I., Puente-Sanchez, F., Tamames, J., Servin-Garciduenas, L.E., Gonzalez-Toril, E., et al., 2022. Metagenomic and metabolic analyses of poly-extreme microbiome from an active crater volcano Lake. Environ. Res. 203, 111862. https://doi.org/10.1016/j.envres.2021.111862.
Petras, D., Koester, I., Da Silva, R., Stephens, B.M., Haas, A.F., Nelson, C.E., et al., 2017. High-resolution liquid chromatography tandem mass spectrometry enables large scale molecular characterization of dissolved organic matter. Front. Mar. Sci. 4, 405. https://doi.org/10.3389/fmars.2017.00405.
Rebouche, C.J., Seim, H., 1998. Carnitine metabolism and its regulation in microorganisms and mammals. Annu. Rev. Nutr. 18, 39–61. https://doi.org/10.1146/annurev.nutr.18.1.39.
Schlitzer, R., 2002. Interactive analysis and visualization of geoscience data with ocean data view. Comput. Geosci. 28 (10), 1211–1218. https://doi.org/10.1016/s0098-3004(02)00040-7.
Shannon, P., Markiel, A., Ozier, O., Baliga, N.S., Wang, J.T., Ramage, D., et al., 2003. Cytoscape: a software environment for integrated models of biomolecular interaction networks. Genome Res. 13 (11), 2498–2504. https://doi.org/10.1101/gr.1239303.
Singh, A., Shannon, C.P., Gautier, B., Rohart, F., Vacher, M., Tebbutt, S.J., et al., 2019. DIABLO: an integrative approach for identifying key molecular drivers from multi-omics assays. Bioinformatics 35 (17), 3055–3062. https://doi.org/10.1093/bioinformatics/bty1054.
Sun, S.J., Liu, Y.C., Weng, C.H., Sun, S.W., Li, F., Li, H., et al., 2020. Cyclic dipeptides mediating quorum sensing and their biological effects in Hypsizygus marmoreus. Biomolecules 10 (2), 298. https://doi.org/10.3390/biom10020298.
Suominen, S., Gomez-Saez, G.V., Dittmar, T., Sinninghe Damsté, J.S., Villanueva, L., 2021. Interplay between microbial community composition and chemodiversity of dissolved organic matter throughout the black sea water column redox gradient. Limnol. Oceanogr. 67 (2), 329–347. https://doi.org/10.1002/lno.11995.
Tang, K., Liu, L., 2023. Bacteria are driving the ocean's organosulfur cycle. Trends Microbiol. 31 (8), 772–775. https://doi.org/10.1016/j.tim.2023.05.003.
Tripp, H.J., Kitner, J.B., Schwalbach, M.S., Dacey, J.W., Wilhelm, L.J., Giovannoni, S.J., 2008. SAR11 marine bacteria require exogenous reduced sulphur for growth. Nature 452 (7188), 741–744. https://doi.org/10.1038/nature06776.
van Galen, C., Barnard, D.T., Stanley, R.J., 2020. Stark spectroscopy of lumichrome: a possible candidate for stand-off detection of bacterial quorum sensing. J. Phys. Chem. B 124 (52), 11835–11842. https://doi.org/10.1021/acs.jpcb.0c09498.
Xiao, S., Chen, J., Shen, Y., Chen, Q., Wang, Y., Li, Y., et al., 2023. Molecular characterization of organic matter transformation mediated by microorganisms under anoxic/hypoxic conditions. Sci. China Earth Sci. 66 (4), 894–909. https://doi.org/10.1007/s11430-022-1080-8.
Xiao, X., Powers, L.C., Liu, J., Gonsior, M., Zhang, R., Zhang, L., et al., 2022. Biodegradation of terrigenous organic matter in a stratified large-volume water column: implications of the removal of terrigenous organic matter in the coastal ocean. Environ. Sci. Technol. 56 (8), 5234–5246. https://doi.org/10.1021/acs.est.1c08317.
Xie, L., Wang, B., Pu, X., Xin, M., He, P., Li, C., et al., 2019. Hydrochemical properties and chemocline of the sansha yongle blue hole in the South China Sea. Sci. Total Environ. 649, 1281–1292. https://doi.org/10.1016/j.scitotenv.2018.08.333.
Yao, P., Wang, X.C., Bianchi, T.S., Yang, Z.S., Fu, L., Zhang, X.H., et al., 2020. Carbon cycling in the world's deepest blue hole. Journal of Geophysical Research-Biogeosciences 125 (2), e2019JG005307. https://doi.org/10.1029/2019jg005307.
Yin, M., Song, J., Duan, L., Yuan, H., Li, X., Peng, Q., 2023. North-south differences in hypoxia and nitrogen cycle of the East China Sea over the last century indicated by sedimentary bacteriohopanepolyols. Chem. Geol. 620, 121340. https://doi.org/10.1016/j.chemgeo.2023.121340.
Zaikova, E., Walsh, D.A., Stilwell, C.P., Mohn, W.W., Tortell, P.D., Hallam, S.J., 2010. Microbial community dynamics in a seasonally anoxic fjord: Saanich inlet, British Columbia. Environ. Microbiol. 12 (1), 172–191. https://doi.org/10.1111/j.1462-2920.2009.02058.x.
Zehr, J.P., Capone, D.G., 2020. Changing perspectives in marine nitrogen fixation. Science 368 (6492), eaay9514. https://doi.org/10.1126/science.aay9514.
Zhou, S., Liu, J., Yao, P., Fu, L., Yang, Z., Zhang, Y., et al., 2023. Unique bacterial communities and lifestyles in deep ocean blue holes: insights from the yongle blue hole (south China sea). Front. Mar. Sci. 10, 1086117. https://doi.org/10.3389/fmars.2023.1086117.
Zhu, W., Lomsadze, A., Borodovsky, M., 2010. Ab initio gene identification in metagenomic sequences. Nucleic Acids Res. 38 (12), e132. https://doi.org/10.1093/nar/gkq275.